Article

Electrical Life Assessment of the Low-Voltage Circuit Breaker (LVCB) Considering Arc Voltage

Zhengjun Liu [1,*] and Li Wang [2]

1   State Key Laboratory of Reliability and Intelligence of Electrical Equipment, Hebei University of Technology, Tianjin 300130, China
2   Key Laboratory of Electromagnetic Field and Electrical Apparatus Reliability of Hebei Province, Hebei University of Technology, Tianjin 300130, China; liwang86@126.com
*   Correspondence: liuzhengjun690@gmail.com

Abstract: The low-voltage circuit breaker (LVCB) is commonly utilized in the distribution network. An accurate evaluation of its electrical life is related to the safety and reliability of electric energy output. The traditional arc erosion model only considers the effect of current on contact wear while ignoring the impact of operation conditions (supply voltage and power factor) on electrical life. As a result of the arc voltage, the original circuit topology changes, resulting in an early current zero. At 220–660 V AC supply voltages, arc voltage causes the distortion of the breaking current waveform, and the contact erosion amount (CEA) is smaller than that in the ideal case. This work investigates the effect of arc voltage on breaking current, develops an arc erosion model that includes arc voltage, and compares the CEA curves for various supply voltages and power factors. The electrical life of the LVCB is then simulated using the Monte Carlo approach to determine the distribution of electrical life under various operating situations. The results reveal that the LVCB's electrical life diminishes as the supply voltage increases under the same power factor; it first declines and then increases as the power factor grows under the same supply voltage. For the combination of two parameters (220 V, 0.95) and (660 V, 0.65), the electrical life difference of the LVCB can reach 21.4%. The method solves the low accuracy problem of the LVCB life assessment under different operation conditions. It improves the efficiency of overhaul and maintenance on the LVCB in power distribution systems.

Keywords: arc voltage; life assessment; low-voltage circuit breaker; arc erosion

1. Introduction

With the development of the economy and the increasing electricity demand, people's requirements for the reliability of modern power systems continue to increase. As an essential safety device in the low-voltage distribution network, the low-voltage circuit breaker (LVCB) plays the role of distributing electric energy and performing on-off operations for low-voltage distribution circuits, motors, or other electrical equipment according to specified conditions [1–3]. An LVCB is an essential electrical device in the entire power supply network, and it is vital to ensure its safe and reliable running during the service stage [4,5].

The electrical life of an LVCB is the number of on-load operations that the device can withstand under the specified on and off conditions without repairing and replacing any parts [6]. The contact wear caused by electrical stress is the main reason for the LVCB's degradation and failure. During the breaking process of the LVCB, an arc is generated between the contacts, which causes mass loss on the contact surface. This mass loss resulting from the arc current is called the contact erosion amount (CEA). When the CEA threshold of the LVCB is reached, the contact performance cannot meet the switch-on requirements, and then it fails [7,8]. The research on the electrical life of the LVCB is the basis for the reliability assessment of the distribution network. LVCBs are extensively equipped in the distribution

network. During the whole life cycle, it is frequently required to design targeted running and maintenance plans, which necessitates a thorough understanding and judgment of the electrical life of LVCBs [9,10].

In terms of electrical life assessment methods for the switching apparatus, some researchers have studied new methods for contact erosion monitoring. The Savitzky–Golay convolution smoothing technique is integrated with the BP neural network algorithm in [11], and the arcing time, arc energy, and arcing phase angle are selected as characteristic parameters. The remaining electrical life prediction model for the contacts is established, which enhances the forecast accuracy over the old methodology. In [12], an electrical life assessment model based on cloud theory is proposed, considering the fuzziness and randomness in life evaluation. This approach uses a cloud model to replace the traditional interval method to divide the insulation state level of the circuit breaker. According to an example calculation analysis, it is demonstrated that the new model is more accurate than the old one. From the perspective of the erosion rate and wear coefficient, an electrical life assessment method for the Cu-W contact of the circuit breaker is proposed [13], which can be used to support the design of arc contacts. Meanwhile, it is noted that the size and type of contacts affect electrical life. In [14], a novel method is proposed for processing time-resolved spectral signals using the chromaticity method. It is applied to the online monitoring of contact erosion in the high-voltage circuit breaker. The time-resolved spectroscopy of the arc is captured using an optical fiber sensor. The spectral emission time is correlated with the contact mass loss and the degree of surface deterioration. In [15], a method for determining the arcing time using auxiliary contacts is proposed, and the test is performed on circuit breakers with different excitation coils. The technique is appropriate for high-voltage gas circuit breakers. The auxiliary contacts can be accessed during the online operation to perform an online assessment of the circuit breaker contact state. The authors of [16] analyze the changing law of characteristics such as arc time, arc energy, and breaking phase angle with the operation numbers of a special AC contactor that is often used in low-voltage power distribution systems. Simultaneously, this study created a database of crucial electrical life features and effectively applied the strategy to electrical fire detection. In [17,18], the corresponding relationship between the dynamic contact resistance of the circuit breaker and the contact erosion state is analyzed, and the related state evaluation methods are proposed. The authors of [19] investigate an online evaluation approach of the high-voltage circuit breaker considering multiple physical parameters. The authors of [20] describe the distribution characteristic of electrical life for AC contactors. The authors of [21] introduce the arc plasma characteristic and arc movement of the LVCB. The influence of reignition is examined on the LVCB in [22]. In addition, there are multiple linear regression-based and arc discharge power-based monitoring algorithms for the CEA of circuit breakers [8,23]. Regardless of the approach used, the goal of the electrical life study of the LVCB is to determine the contact erosion degree and provide a baseline for the overall performance degradation of the switching apparatus. It is still an effective method to use arc energy to characterize the contact erosion state.

In the study of the arc erosion mechanism of the switching apparatus, three key considerations are electrical, contact, and equipment parameters [24–27]. Electrical parameters include arc energy, breaking current level, arcing phase angle, arcing time, and electric charge. Contact parameters include material properties, processing technology, and geometry shape. Breaking speed, opening distance, arc extinguishing mode, and arc extinguishing medium are examples of equipment parameters. Additionally, [28] investigates the effect of operation frequencies on arc erosion behavior. The surface morphology, microstructure, and element distribution of the Ag/CdO contact are described utilizing scanning electron microscopy. Furthermore, the formation process and action mechanism of arc erosion are analyzed. In [29,30], the influence of alloying elements and the manufacturing process on the arc erosion characteristics of contact materials are studied, respectively. The authors of [31] analyze the effect of load characteristics on contact erosion behavior.

Despite the availability of several state evaluation techniques for on-site diagnosis and testing of the switching apparatus, there are still some problems in the electrical life assessment of the LVCB. First, due to the limitation of the circuit breaker structure and detection cost in the low-voltage field, the LVCB maintenance is mainly periodic, without considering the impact of the operation environment, which will lead to excessive or insufficient maintenance. Second, the existing arc erosion model usually only considers the influence of current when calculating the CEA and takes the arc current waveform as a standard sine wave. However, in actual operation, the current waveform of the LVCB changes with the power factor and supply voltage, which makes the theoretical estimated value quite different from the actual value of electrical life. Therefore, this paper studies the arc erosion law of the LVCB considering the arc voltage and analyzes the electrical life distribution features of the LVCB under different supply voltages and power factors.

Due to the influence of arc, the circuit topology changes, the waveform of breaking current is distorted, and the zero-crossing of arc current is early (compared with the current before contact separation). Therefore, the maximum current and arcing time change with t_0. Firstly, this paper examines the motion law of arc voltage during the breaking process and establishes the arc voltage mathematical model of the LVCB based on arc starting time. Then, the arc erosion model considering arc voltage is established. The arc current waveform and contact wear curve variations of the LVCB under different supply voltages and power factors are obtained. At the same time, the electrical life simulation test is carried out with the help of the Monte Carlo approach, and the LVCB's electrical life distribution is obtained. Finally, the effectiveness of this method is compared and analyzed through experiments. Research on this subject can help increase the accuracy of lifetime evaluation under various loads and operation conditions while also serving as a technical reference for the LVCB's reliability evaluation and running and maintenance plan.

The remainder of this research is organized as follows: Section 2 presents an arc voltage model that is based on the arc starting time (AST). Section 3 analyzes the arc current of the LVCB. Section 4 establishes an arc erosion model for the LVCB considering arc voltage and analyzes the arc erosion variation under different supply voltages and power factors. Section 5 conducts electrical life simulation experiments by the Monte Carlo method. Section 6 verifies the validity of the method by electrical life test. In Section 7, the conclusion is provided.

2. Arc Voltage Model of the LVCB Based on AST

In order to study the influence of supply voltage and power factor on electrical life, it is necessary to establish an arc erosion model with the help of arc voltage. The first thing to do is analyze the variation law of arc voltage during contact breaking. The arc of the LVCB consists of three parts: near-cathode zone, near-anode zone, and arc column zone. Similarly, the arc voltage is also divided into cathode voltage drop, anode voltage drops, and arc column voltage drop. The essence of the electrode voltage drop is the space charge excited by the electric field between the contacts, which is closely related to the material on the contact surface and the gas medium. For air medium, the value of cathode voltage drop is close to that of anode voltage drop. When the arc burns steadily, the voltage drop between the cathode and anode fluctuates less as the current varies and can be approximated as a constant. For the arc column zone, the essence of the arc column voltage drop is the ionization of air to form plasma, which is closely related to the electric field strength and arc length. The arc voltage u_e can be approximately expressed as:

$$u_e = u_c + u_a + u_z = u_0 + El, \tag{1}$$

where u_c is the cathode voltage drop, u_a is the anode voltage drop, u_z is the arc column voltage drop, u_0 is the electrode voltage drop, E is the arc column electric field strength, and l is the arc length.

By analyzing the I-V characteristic curve of the AC arc, the relationship between the arc voltage and the current of the LVCB has been apparent. However, in the analysis and

calculation of the electrical life, people are concerned about the erosion effect of the current on the contact during a specific arcing time, and the corresponding arc starting time (AST) is an essential physical quantity. The AST of an LVCB refers to the time interval from the arc burning moment to the previous current zero. Its distribution interval is [0, T/2), where T is the circuit period. With the aid of the AST concept, the relationship between contact breaking operation and arc voltage of the LVCB can be established, which lays a foundation for the subsequent analysis of electrical life characteristics.

For investigating the arc voltage variation of the LVCB based on the AST, it is necessary to analyze the movement characteristics during the contact breaking of the LVCB. It cannot cause damage to the parts while ensuring the quick action of the contacts. Assume that the AST is t_0, the breaking speed is v, the contact opening distance is D, and the contact gap is d during the breaking process. There are three situations to describe the relationship among t_0, d, and D.

- t_0 is a large number. The contact gap d does not reach the opening distance D when the arc reaches the zero-crossing point and extinguishes, and the contact keeps moving after the arc is extinguished;
- t_0 is moderate. When the arc is extinguished, the contact gap $d = D$;
- t_0 is relatively small. Before the arc is extinguished, the contact gap has reached D, and it remains unchanged as the arc burns until the arc is extinguished.

The second case is a particular case of contact breaking. That is, the contact gap is exactly D when the arc is extinguished, and the AST is t_D at this time, then the variation law of the contact gap can be obtained as follows:

$$d(t_0 < t_D) = \begin{cases} vt, & t \in [0, \frac{T}{2} - t_D) \\ D, & t \in [\frac{T}{2} - t_D, \frac{T}{2} - t_0] \end{cases}, \tag{2}$$

$$d(t_0 \geq t_D) = vt, \quad t \in [0, \frac{T}{2} - t_0], \tag{3}$$

Equations (2) and (3) show that the change of the contact gap is closely related to the AST. Combined with Equation (1), the arc voltage can be written as a functional curve cluster related to t_0 during the contact separation. According to the changing characteristics of the arc voltage, the arc voltage value reaches the maximum when the arc is extinguished. The maximum arc voltage can be expressed as Equation (4).

$$u_{\max} = \begin{cases} u_0 + ED, & t_0 \in [0, t_D] \\ u_0 + Ev(\frac{T}{2} - t_0), & t_0 \in [t_D, \frac{T}{2}) \end{cases}, \tag{4}$$

When the contact gap changes little during the initial stages of contact breaking, it can be assumed that the gap between contacts rises linearly with time. The variation of arc voltage with the AST obtained according to Equation (4) is shown in Figure 1. Since the AC arc has negative resistance characteristics and the arc voltage is practically constant while the arc is burning stably, the average value of the arc voltage during contact breaking is utilized to indicate the overall fluctuation features of the arc voltage. The blue curve in Figure 1 shows the corresponding relationship between the maximum arc voltage (at the arc extinction point) and the AST, i.e., t_0-$u_{\max}$. The red curve indicates the corresponding relationship between the mean value u_e^* of arc voltage and the AST. Because the arc voltage in the arc burning section increases first and then tends to be stable, and the average arc voltage is less than the voltage at the arc extinguishing point, the curve inflection point is advanced. Without special instructions, the arc voltage in the following paper is the average arc voltage value.
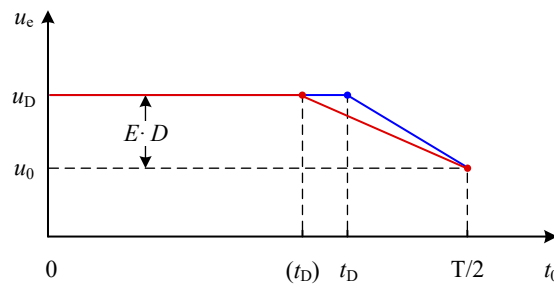
Figure 1. Relationship between arc voltage and AST.

The corresponding relationship between u_e^* and t_0 is established from Figure 1, as shown in Equation (5):

$$u_e^* = \begin{cases} u_D, & 0 \le t_0 < t_D \\ \frac{2}{T-2t_D}[-(u_D - u_0)t_0 + \frac{T}{2}u_D - t_D \cdot u_0], & t_D \le t_0 < \frac{T}{2} \end{cases} , \tag{5}$$

Equation (5) shows that the key to determining the link between the arc voltage and the AST is to discover the values of the three parameters t_D, u_0, and u_D. u_0 and u_D are the near-pole voltage drop and the arc voltage value during stable arcing, respectively, which are determined by the contact material and the opening distance. t_D is the inflection point of the voltage curve, which is also related to the characteristics of the circuit breaker itself. In the same batch of the LVCB, the parameters of t_D, u_0, and u_D can be considered unchanged.

To estimate the parameter values for t_D, u_0, and u_D, we can consult the relevant data of the LVCB contact material and contact travel curve. Furthermore, the three parameters may be computed by collecting the arc current and voltage waveform under various AST. This paper collected the arc voltages at different ASTs, and the average voltage is calculated. The results are shown in Figure 2.
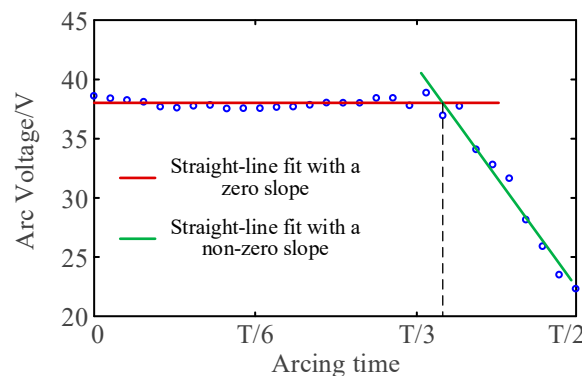

Figure 2. The average value of arc voltage at different AST.

After curve fitting, it can be obtained that u_0 = 22 V, u_D = 38 V, t_D = 0.36 T.

3. Arc Current Waveform of the LVCB

The analysis of the arc current waveform of the LVCB is the basis for establishing the arc erosion model. In the low-voltage switching apparatus field, the traditional arc erosion model considers that the arc current is the same as the steady-state current of the power system when the contact is broken. If the breaking current level does not change, the electrical life of the LVCB remains unchanged. The arc current is shown in Equation (6).

$$i = \sqrt{2}I\sin[\omega(t + t_0)], \tag{6}$$

However, Equation (6) cannot account for the effect of voltages and power factors on electrical life. According to actual operating data, the electrical life of the LVCB is also

highly connected with the supply voltage and power factor. After introducing the arc voltage, changes of arc current under different supply voltages and power factors and the influence on the CEA can be obtained. The specific analysis process is given below. Using a single-pole contact as an example, Figure 3 shows the equivalent circuit diagram of a contact-breaking load circuit. Among them, R and L are load-side resistance and inductance, which can be used to adjust the circuit power factor. C is the capacitance to the ground, and the current flowing through C is usually minimal, and its current value can be ignored. u_p and u_e are the supply voltage and arc voltage, respectively.
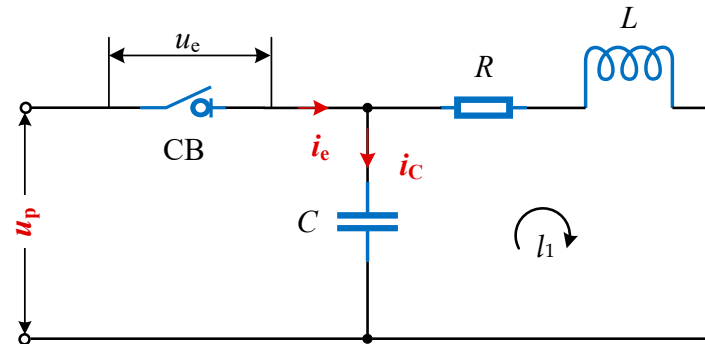

Figure 3. Equivalent circuit diagram of the contact breaking load circuit.

After the contacts of the LVCB are separated, an arc is generated between the contacts. The existence of the arc changes the original structure of the circuit. For the LVCB, on the one hand, the existence of the arc voltage plays a role in limiting the current, and on the other hand, the factors affecting the electrical life become more complicated. According to Figure 3, the voltage equilibrium equation is as follows:

$$Ri_e + L\frac{di_e}{dt} + u_e = \sqrt{2}U\sin[\omega(t + t_0) + \theta], \tag{7}$$

From Equation (7), the arc current can be obtained as:

$$i_e(t) = Ae^{-Rt/L} + \frac{B}{\omega}\sin[\omega(t + t_0) + \theta] - \frac{BL}{R}\cos[\omega(t + t_0) + \theta] - \frac{u_e}{R}, \tag{8}$$

where U is the supply voltage RMS, θ is the power factor angle, and ω is the angular frequency of the AC power supply. The initial condition is i_e ($t = 0$, $t_0 = 0$) = 0. $A = \frac{BL}{R}\cos\theta - \frac{B}{\omega}\sin\theta + \frac{u_e}{R}$, $B = \frac{\sqrt{2}UR\omega}{R^2 + \omega^2 L^2}$.

3.1. Arc Current Waveform under Different ASTs

According to Equation (8), the arc current waveforms at different ASTs are obtained in Figure 4. In Figure 4, the supply voltage is 220 V, the current RMS is 10 A, the power factor is 0.65, and the frequency is 50 Hz.

The arc current is not a standard sine wave throughout the contact breaking process, as seen in Figure 4, and the current amplitude fluctuates with the AST. Furthermore, the arc extinguishing time is not fixed at T/2. The greater the arc starting time t_0, the closer the arc extinguishing time is to T/2. The smaller the arc starting time is, the greater the difference between the arc current amplitude and the ideal current amplitude is.
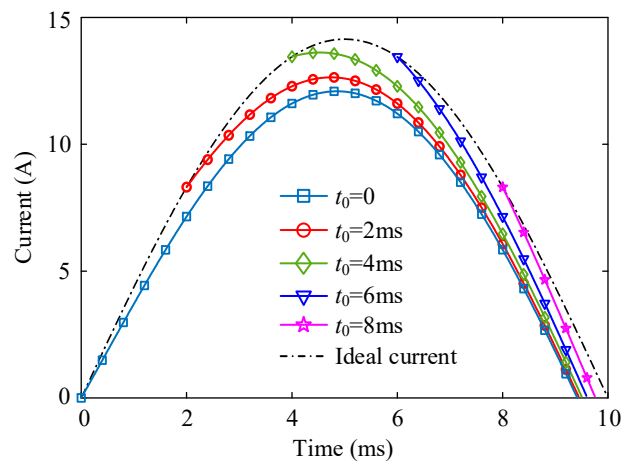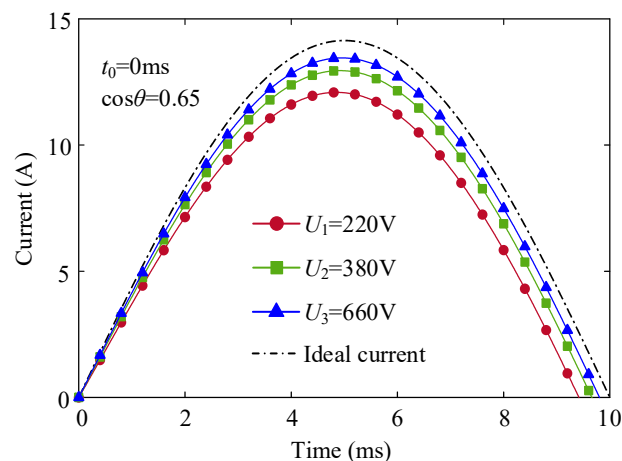
Figure 4. Arc current waveform under different ASTs.

3.2. Arc Current Waveform under Different Supply Voltages

In order to analyze the influence of supply voltage on arc current waveform, three different supply voltages are selected in this paper: 220 V, 380 V, and 660 V. The arc current waveform obtained under different supply voltages is shown in Figure 5.
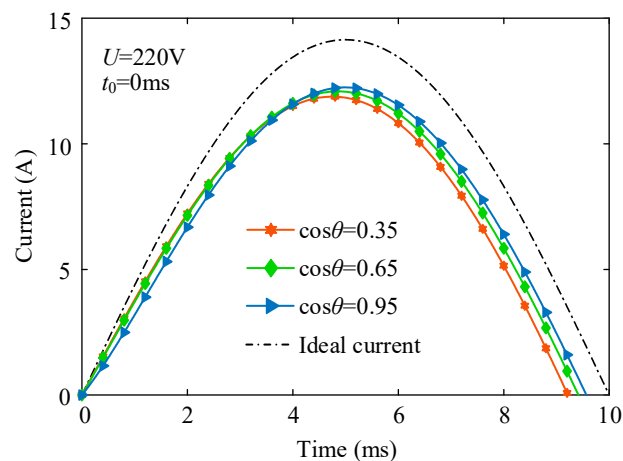

Figure 5. Arc current waveform under different supply voltages.

t_0 and the power factor in Figure 5 are fixed. The dotted line is the current waveform under ideal conditions. From the arc current waveform, when t_0 = 0 ms, it can be obtained that the larger the supply voltage, the larger the current amplitude at the same AST, and the longer the arcing time. It can be preliminarily judged that with the increasing supply voltage, the erosion effect of the arc on the contacts is more significant. Meanwhile, the electrical life of the LVCB is decreasing, which is consistent with the actual usage.

3.3. Arc Current Waveform under Different Power Factors

For investigating the effect of power factors on arc current, this paper selects three power factors of 0.35, 0.65, and 0.95 to examine the variation law of arc current. Taking the AST t_0 = 0 ms and the supply voltage as 220 V as an example, the arc current waveform under different power factors is obtained, as shown in Figure 6.

Figure 6. Arc current waveform under different power factors.

As shown in Figure 6, the power factor is different, and the arc current waveform is different. The higher the power factor, the longer the arcing time. However, unlike the effect of the supply voltage on the arc current amplitude, the arc current amplitude decreases with the increasing power factor before $t_0 = 4$ ms. After 4 ms, the arc current amplitude increases as the power factor increases. As a result, the changing trend of the CEA is not entirely consistent with the trend of the power factor, and the impact of the power factor on the CEA must be considered comprehensively in conjunction with the AST.

4. Arc Erosion Model of the LVCB Considering Arc Voltage

The arc erosion model of the LVCB characterizes the corresponding relationship between erosion quality and arc current [6,12]. By establishing an arc erosion model, the electrical life of the LVCB can be simulated effectively. While saving costs, it can also significantly improve work efficiency. The CEA considering arc voltage under a single contact operation is obtained through the arc current integration during the arcing time, as shown in Equation (9):

$$q_e = \int_0^{\Delta t} f(i_e)dt, \tag{9}$$

where Δt is the arcing time. The function $f(i_e)$ can be represented by $|i_e|$ or i_e^2. The contact erosion of each operation is calculated by Equation (9). Then, the remaining electrical life of the switching apparatus can be obtained according to the appropriate threshold setting to achieve the purpose of evaluating the electrical life. Considering the present research results, if the breaking current level is not high (<1 kA), $i_e^2 t$ can be selected as a characterization equation of arc erosion.

4.1. Variation of CEA with Supply Voltage

The study of the change law of CEA with the AST can further analyze the characteristics of supply voltage effect on the electrical life of the LVCB. The CEA curve under different supply voltages is analyzed by Equation (9). The power factor is fixed at 0.65. The CEA curve is shown in Figure 7.

The black curve in Figure 7 is the change rule of the CEA when the arc voltage is not considered (referred to as the erosion curve in the ideal situation). With the increasing AST, the CEA gradually decreases. The other three curves are the change waveforms of the arc erosion amount after considering the arc voltage. The greater the supply voltage, the closer the CEA change curve is to the ideal situation. In addition, the CEA curve does not always show a decreasing trend but increases first and then decreases, which brings a new explanation to the traditional contact erosion law (the longer the arcing time is, the greater the CEA of the LVCB). This phenomenon is because the maximum current decreases while arcing time increases in the t_0 range of 0–2 ms.
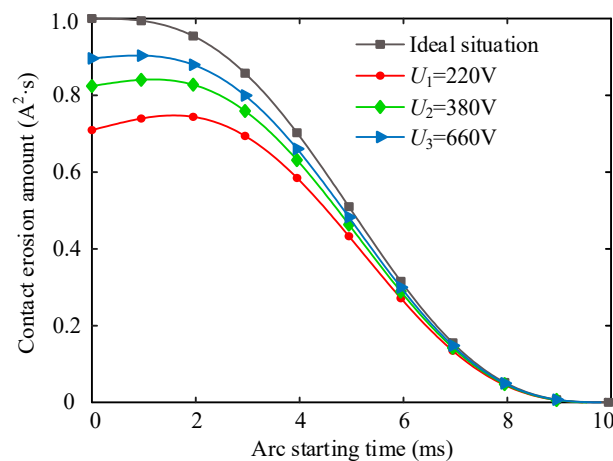
Figure 7. CEA curve with AST under different supply voltages.

As a result, two conclusions may be taken just from the standpoint of the impact of the supply voltage on electrical life. One is that the electrical life test of the low-voltage switching apparatus is carried out before leaving the factory, and the electrical erosion of the contacts is smaller than that obtained by i^2 integration under ideal conditions. The electrical life is significantly longer than the theoretical calculation. Second, the higher the supply voltage in actual running, the greater the CEA of the LVCB. It is also true that the electrical life of the LVCB is shorter with a high supply voltage than a low one, despite the same breaking current level.

In addition, by observing the change curve of the CEA, it can be found that when the supply voltage is low, the maximum CEA is around 2 ms. Consequently, it can be concluded that if the AST is approximately 2 ms, the electrical life is reduced accordingly. This finding should be considered while researching the link between AST distribution and the electrical life and when constructing the breaking control signal of the intelligent circuit breaker.

4.2. Variation of CEA with Power Factor

By Equation (9), the CEA curve in a single operation with the AST for various power factors is obtained, as shown in Figure 8. The CEA change curves under different power factors show the crossing phenomenon, and the intersections of the three curves are different. After $t_0 = 3$ ms, the CEA and the power factors have the same change trend. To further analyze the effect of the power factor, this paper integrates the CEA curve in the range of [0, T/2) and takes the average CEA. It takes the average value to calculate the CEA under different power factors. The curve of the average CEA is shown in Figure 9.
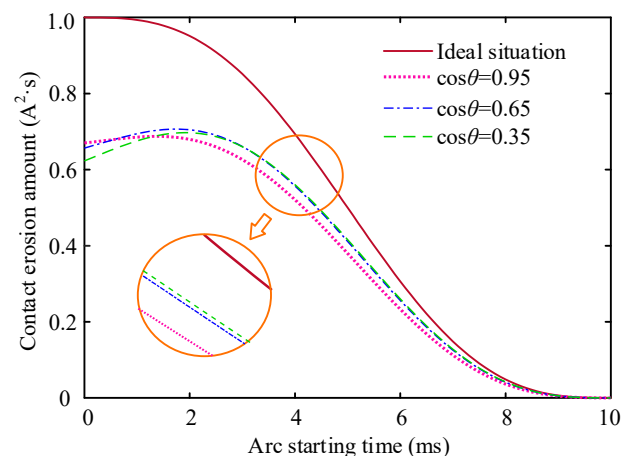
Figure 8. CEA curve of single operation with the AST.
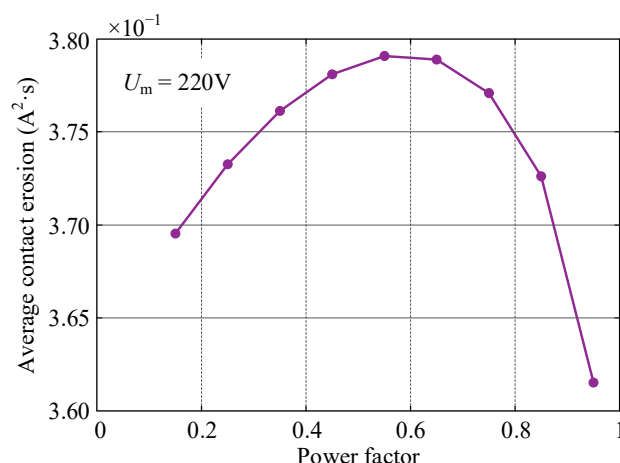
Figure 9. Average CEA curve under different power factors.

Figure 9 shows that the average CEA does not increase or decrease linearly with the increasing power factor. The change curve is arched, and the maximum value is around 0.6. It shows that for the switching apparatus whose AST is randomly distributed, the CEA of the LVCB is the largest at this time, which also explains the difference in the electrical life of the LVCB under different loads.

5. Simulation of the LVCB Electrical Life

5.1. Simulation Process of the Electrical Life Test

The Monte Carlo approach is used in this article to simulate the electrical life process. The electrical life of the LVCB is compared under two conditions: the ideal case and the scenario where the arc voltage is considered. With the aid of the arc erosion model considering arc voltage, the electrical life histogram of the LVCB under different supply voltages and power factors is obtained. The AST is assumed to be evenly distributed in the interval [0, T/2]. The main parameters of the simulation are shown in Table 1.

Table 1. Electrical life simulation test parameters.

Current/A	Frequency/Hz	Supply Voltage/V	Power Factor
10	50	220	0.35/0.65/0.95
		380	0.35/0.65/0.95
		660	0.35/0.65/0.95

According to the damage accumulation effect, the contact fails when the CEA reaches the CEA threshold Q. We take the single-pole LVCB as an example, and the average electrical life is 10,000. According to Equation (9), the average CEA is $q^* = \pi I^2(2\omega)$ in ideal conditions, and the circuit current is 10 A, then $Q = q^* \times 10,000 = 0.5 \times 10,000 = 5000$ (A^2·s).

The simulation process of the contact electrical life test is as follows:

1. A random number t_0 subject to uniform distribution is generated in the interval [0, T/2];
2. The CEA is calculated according to Equation (9);
3. The accumulated CEA, M of the contact is calculated. $M < Q$, repeat steps 1–3. $M \geq Q$, terminate the test and record the electrical life of the contacts;
4. The above process is repeated k times independently to obtain the distribution of the electrical life of k samples.

The simulation flow chart is shown in Figure 10.
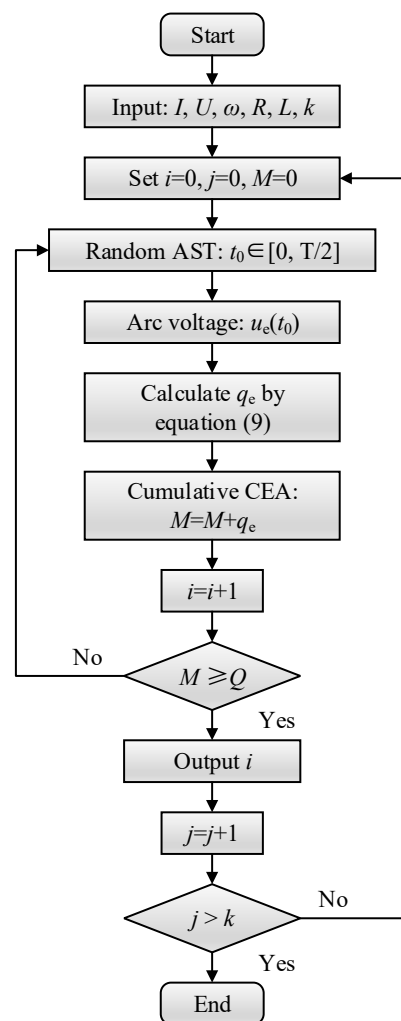
Figure 10. Simulation flow chart of electrical life.

5.2. Results of the Simulation

    Statistical analysis is carried out on the electrical life obtained by the simulation. The histogram of the LVCB electrical life under various supply voltages and power factors is shown in Figure 11.

    It can be seen from Figure 11 that even at the same breaking current level, the electrical life of the LVCB is not fixed but changes with the supply voltage and power factor. The median of the electrical life distribution histogram of the LVCB is counted. The maximum electrical life combination is (220 V, 0.95), and the minimum electrical life combination is (660 V, 0.65). The percentage difference in electrical life between the two is 21.4%.

    When the supply voltage is 220 V, the difference in the electrical life of the LVCB among the three power factors is 3.8%; similarly, when the supply voltage is 380 V and 660 V, the values are 2.0% and 1.1%. When the power factor is set to 0.35, the difference percentage of the electrical life of the LVCB among the three supply voltages is 17.6%; when the power factor is set to 0.65 and 0.95, respectively, the percentage of electrical life difference is 17% and 20.1%.

    It shows that under the same supply voltage level, the electrical life of the LVCB near the power factor of 0.65 is the smallest. With the increasing supply voltage level, the effect of power factors on the electrical life of the LVCB continues to decrease. The electrical life of the LVCB is inversely proportional to the supply voltage under the same load. Furthermore, the effect of supply voltage on the electrical life is the largest when the power factor is 0.95 and decreases in turn when the power factor is 0.35 and 0.65. Therefore, in actual
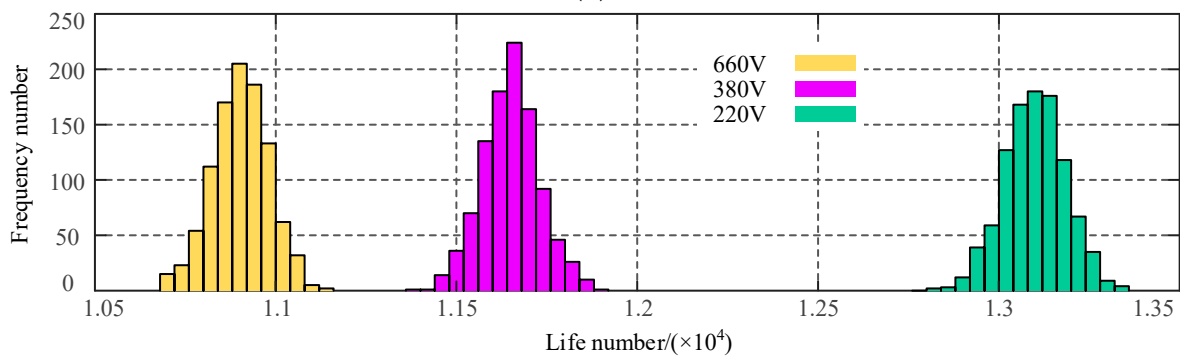
running, the changes between the two sets of parameters should be comprehensively considered, and the electrical life of the LVCB should be accurately evaluated.
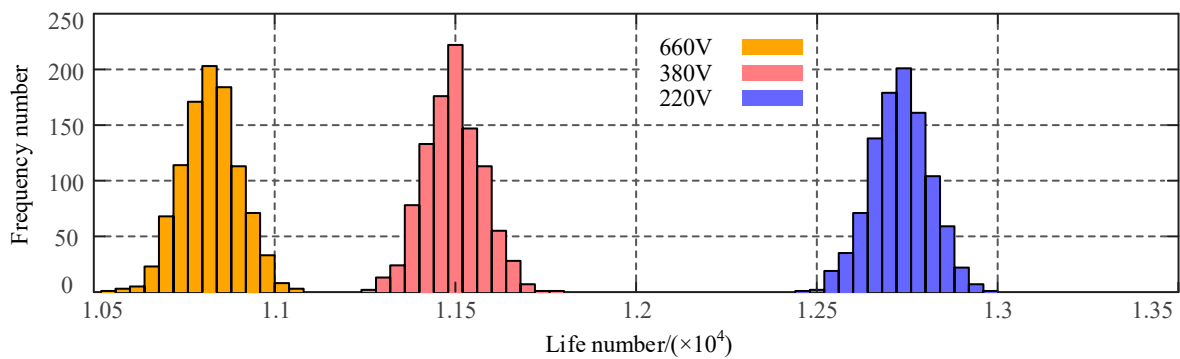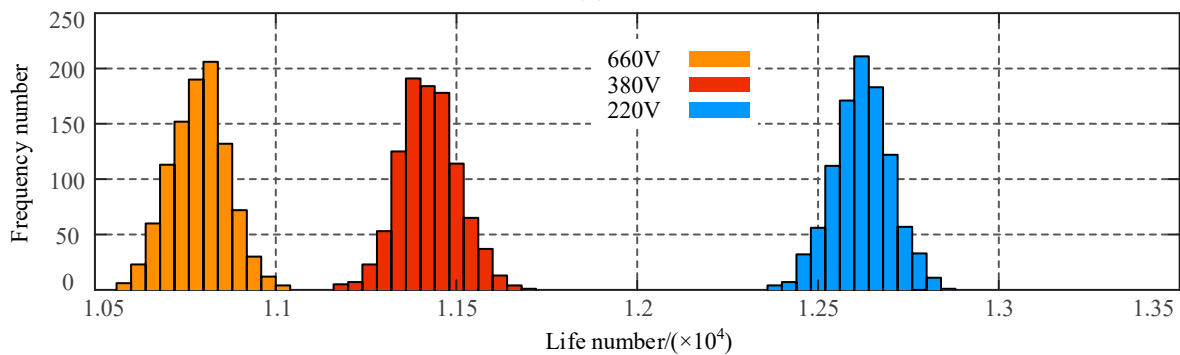
Figure 11. Histogram of electrical life distribution. (**a**) Electrical life distribution under different supply voltages when power factor is 0.35; (**b**) electrical life distribution under different supply voltages when power factor is 0.65; (**c**) electrical life distribution under different supply voltages when power factor is 0.95.

6. Experimental Validation

An LVCB electrical life test is designed to verify the effectiveness of this method. The switch model is DZ47-63, the rated voltage is 415 V, and the test current is 10 A. The selected parameter combination is (220 V, 0.35/0.65/0.95), (380 V, 0.65). Figure 12 illustrates the electrical life test device, and the collected voltage and current waveforms are shown in Figure 13.
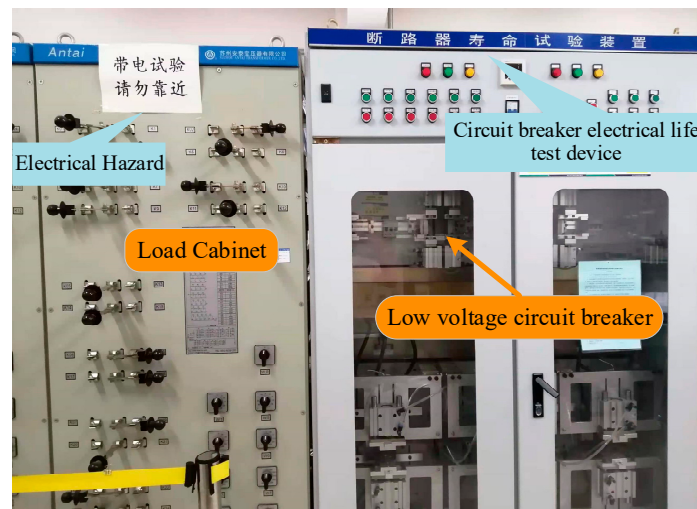
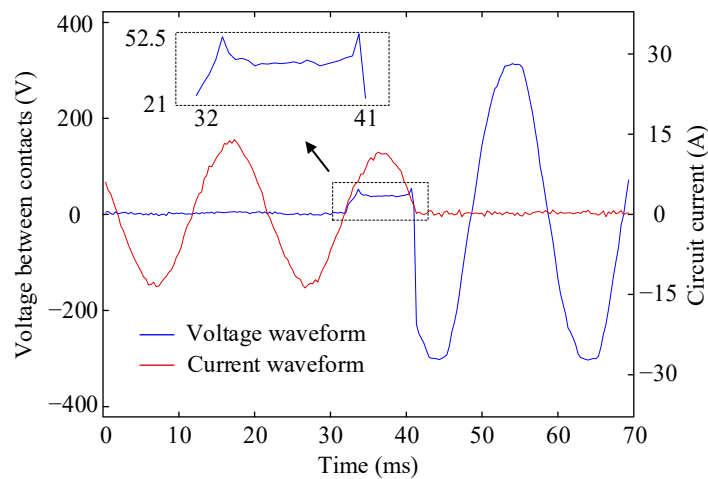**Figure 12.** The electrical life test device.

Figure 13. Voltage and current waveforms.

According to the sampling points of the arc current, the CEA at different ASTs is calculated and compared with the change curve of the CEA obtained by simulation, as shown in Figure 14. The supply voltage is set to 220 V, and the power factor is 0.65. Figure 14 shows that after considering the arc voltage, the change curve of the CEA is closer to the actual value.
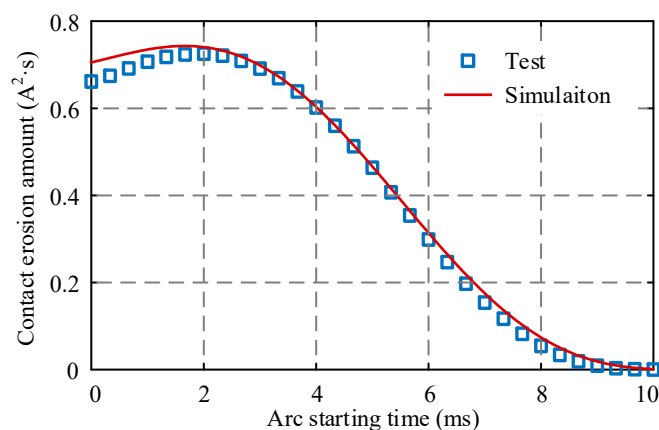

Figure 14. Contact erosion amount curve.

Because there is a particular deviation in the electrical life of different LVCB samples, this paper uses the concept of relative remaining life to compare the similarities and differences between the life changes obtained by testing and simulation under different parameters. For the LVCB with evenly distributed ASTs, the relative remaining life equation is as follows:

$$L = 1 - \sum_{j=1}^{N} \frac{q_j}{Q} = 1 - \frac{q^* N}{Q}, \tag{10}$$

When the life of the LVCB ends, $N = Q/q^*$. For the LVCB with the same threshold, q^* is inversely proportional to Q.

In this paper, four sets of parameter combinations are selected for testing. The CEA threshold is 5000 ($A^2 \cdot s$) according to Section 5.1. After calculation, the electrical life of the LVCB under different parameter combinations is shown in Table 2.

Table 2. The electrical life of the LVCB under different parameters.

N	Parameter Combination			
	(220, 0.35)	**(220, 0.65)**	**(220, 0.95)**	**(380, 0.65)**
Simulation	12,731	12,621	13,098	11,424
Test	13,501	13,198	13,930	12,074

Due to the existence of line resistance and inductance during actual operation, the current-limiting impact of the LVCB is greater than the theoretical analysis value. The actual electrical life in Table 2 is slightly longer than the simulation life. However, the change law of electrical life between the two cases is similar, indicating that simulations can be used to evaluate life under different operation conditions in the future.

7. Conclusions

We propose an arc erosion model considering arc voltage to assess the electrical life of the LVCB in distribution networks. The model can improve the prediction accuracy for the electrical life of LVCBs at different supply voltages and power factors. In the low-voltage power distribution system, the electrical life assessment of switchgear is usually complicated and cumbersome due to the limitation of cost and area. The traditional arc erosion model can only reflect the influence of breaking current levels on electrical life. Supply voltage and power factors cannot be taken into account. With the addition of arc voltage to the arc erosion model, the effect of the arc on breaking current waveforms can be analyzed. According to the change mechanism of arc current in the breaking circuit, we carry out electrical life simulation and test verification and analyze the results. Under the same CEA threshold, the higher the supply voltage level, the smaller the electrical life. Power factor 0.6 has the shortest electrical life among the same supply voltage. This method can theoretically provide an overall understanding and mastery of the electrical life of the LVCB, thereby improving work efficiency and ensuring the safe operation of the power grid. At the same time, the research results can also provide a reference for the research on the existing operation and maintenance strategies of the LVCB.

Data Availability Statement: Not applicable.

Conflicts of Interest: The authors declare no conflict of interest.

References

1. Sidhu, H.; Goel, N.; Chacko, S. Selection of Optimum Circuit Breaker for a Low-Voltage Industrial Power Distribution System. In Proceedings of the 2021 7th International Conference on Electrical Energy Systems (ICEES), Chennai, India, 11–13 February 2021; pp. 89–94.
2. Shu, L.; Wu, Z.; You, Y.; Dapino, M.J.; Zhao, S. Design and Adaptive Control of Matrix Transformer Based Indirect Converter for Large-Capacity Circuit Breaker Testing Application. *IEEE Trans. Ind. Electron.* **2020**, *68*, 5314–5324. [CrossRef]
3. Li, C.; Wei, D.; Zhang, B.; Li, J.; Zhang, W. On novel methods for characterizing the arc/contact movement and its relation with the current/voltage in low-voltage circuit breaker. *IEEE Trans. Plasma Sci.* **2017**, *45*, 882–888. [CrossRef]
4. Subramaniam, A.; Sahoo, A.; Manohar, S.S.; Raman, S.J.; Panda, S.K. Switchgear Condition Assessment and Lifecycle Management: Standards, Failure Statistics, Condition Assessment, Partial Discharge Analysis, Maintenance Approaches, and Future Trends. *IEEE Electr. Insulat. Mag.* **2021**, *37*, 7–41. [CrossRef]
5. Hoffmann, M.W.; Wildermuth, S.; Gitzel, R.; Boyaci, A.; Gebhardt, J.; Kaul, H.; Amihai, I.; Forg, B.; Suriyah, M.; Leibfried, T. Integration of novel sensors and machine learning for predictive maintenance in medium voltage switchgear to enable the energy and mobility revolutions. *Sensors* **2020**, *20*, 2099. [CrossRef]
6. Li, K.; Zhao, C.; Niu, F.; Zheng, S.; Duan, Y.; Huang, S.; Wu, Y. Electrical performance degradation model and residual electrical life prediction for AC contactor. *IEEE Trans. Compon. Pack. Manuf. Technol.* **2020**, *10*, 400–417. [CrossRef]
7. Sun, S.; Wen, Z.; Du, T.; Wang, J.; Tang, Y.; Gao, H. Remaining Life Prediction of Conventional Low-Voltage Circuit Breaker Contact System Based on Effective Vibration Signal Segment Detection and MCCAE-LSTM. *IEEE Sens. J.* **2021**, *21*, 21862–21871. [CrossRef]
8. Feizifar, B.; Usta, O. A novel arcing power-based algorithm for condition monitoring of electrical wear of circuit breaker contacts. *IEEE Trans. Power Deliv.* **2018**, *34*, 1060–1068. [CrossRef]
9. Petrović, I.; Glavaš, H.; Noskov, R.; Blažević, D. Real-Time Circuit Breaker Availability Assessment in the Transmission Network. *Appl. Sci.* **2021**, *11*, 9635. [CrossRef]
10. Wang, L.; Liu, H.; Zheng, W.; Ge, C.; Guan, R.; Chen, L.; Jia, S. Numerical Simulation of Impact Effect of Internal Gas Pressure on Chamber Housing in Low-Voltage Circuit Breaker. *IEEE Trans. Compon. Pack. Manuf. Technol.* **2017**, *4*, 632–640. [CrossRef]
11. Mohammadhosein, M.; Niayesh, K.; Shayegani-Akmal, A.A.; Mohseni, H. Online Assessment of Contact Erosion in High Voltage Gas Circuit Breakers Based on Different Physical Quantities. *Power Deliv. IEEE Trans.* **2018**, *34*, 580–587. [CrossRef]
12. Zheng, S.; Niu, F.; Li, K.; Huang, S.; Liu, Z.; Wu, Y. Analysis of electrical life distribution characteristics of AC contactor based on performance degradation. *IEEE Trans. Compon. Pack. Manuf. Technol.* **2018**, *8*, 1604–1613. [CrossRef]
13. Liu, Z.; Huang, S.; Zhao, C. Study on the Influence of Reignition on Electrical Life Distribution of Low-Voltage Circuit Breakers. *IEEE Access* **2021**, *9*, 91500–91511. [CrossRef]
14. Su, J. Research on Electrical Life Trace Prediction of Contact Based on SG-BP Algorithm. *J. Phys. Conf. Ser.* **2021**, *1952*, 032035. [CrossRef]
15. Hu, C.; Tao, F.; Yang, J.; Liang, Y.; Wang, Y. An assessment method for electrical life of vacuum circuit breaker based on cloud model. In Proceedings of the 2014 ICHVE International Conference on High Voltage Engineering and Application, Pozan, Poland, 8–11 September 2014; pp. 1–4.
16. Ding, C.; Li, C.; Yuan, Z.; Fang, C. An estimation method of Cu-W arcing contact electrical life of SF 6 circuit breakers in making capacitor bank. In Proceedings of the 2019 IEEE Holm Conference on Electrical Contacts, Milwaukee, WI, USA, 14–18 September 2019; pp. 101–107.
17. Wang, Z.; Jones, G.R.; Spencer, J.W.; Wang, X.; Rong, M. Spectroscopic On-Line Monitoring of Cu/W Contacts Erosion in HVCBs Using Optical-Fibre Based Sensor and Chromatic Methodology. *Sensors* **2017**, *17*, 519. [CrossRef] [PubMed]
18. Mohammadhosein, M.; Niayesh, K.; Shayegani Akma, A.A.; Mohseni, H. Online non-invasive evaluation of arcing time for condition assessment of high-voltage gas circuit breakers. *IET Gener. Transm. Distrib.* **2021**, *15*, 1013–1020. [CrossRef]
19. Su, J.; Kang, J.; Lin, C. Electrical Life Test of Small Shell Type Special Contactor and Analysis of Change Trend of Key Characteristics. *J. Phys. Conf. Ser.* **2021**, *1952*, 032017. [CrossRef]
20. Cheng, T.; Gao, W.; Liu, W.; Li, R. Evaluation method of contact erosion for high voltage SF6 circuit breakers using dynamic contact resistance measurement. *Electr. Power Syst. Res.* **2018**, *163*, 725–732. [CrossRef]
21. Freton, P.; Gonzalez, J.-J. Overview of current research into low-voltage circuit breakers. *Open. Plasma Phys. J.* **2009**, *2*, 105–119. [CrossRef]
22. Abdollah, M.; Razi-Kazemi, A.A. Intelligent failure diagnosis for gas circuit breakers based on dynamic resistance measurements. *IEEE Trans. Instrum. Meas.* **2018**, *68*, 3066–3077. [CrossRef]
23. Liu, Y.; Chen, D.; Diao, M.; Xiao, G.; Yan, J.; Wang, Z. Arc contacts ablation state assessment method based on machine learning multiple linear regression. In Proceedings of the International Conference on Mechanical Engineering, Measurement Control, and Instrumentation, Kolkata, India, 8–10 January 2021; pp. 947–952.

24. Shea, J.J. High current AC break arc contact erosion. In Proceedings of the 54th IEEE Holm Conference on Electrical Contacts, Orlando, FL, USA, 27–29 October 2008; pp. xxii–xlvi.

25. Mohammadhosein, M.; Niayesh, K.; Akmal, A.A.S.; Mohseni, H. Impact of surface morphology on arcing induced erosion of CuW contacts in gas circuit breakers. In Proceedings of the 2018 IEEE Holm Conference on Electrical Contacts, Albuquerque, NM, USA, 14–18 October 2018; pp. 99–105.

26. Hwang, S.; Hwang, D.; Baek, H.; Shin, C. Effect of Copper-Based Spring Alloy Selection on Arc Erosion of Electrical Contacts in a Miniature Electrical Switch. *Met. Mater. Int.* **2021**, *27*, 2369–2377. [CrossRef]

27. Shen, F.; Ke, L.-L. Numerical study of coupled electrical-thermal-mechanical-wear behavior in electrical contacts. *Metals* **2021**, *11*, 955. [CrossRef]

28. Wu, Q.; Xu, G.; Yuan, M.; Wu, C. Influence of operation numbers on arc erosion of Ag/CdO electrical contact materials. *IEEE Trans. Compon. Pack. Manuf. Technol.* **2020**, *10*, 845–857. [CrossRef]

29. Wu, C.-P.; Yi, D.-Q.; Wei, W.; Li, S.-H.; Zhou, J.-M. Influence of alloy components on arc erosion morphology of Ag/MeO electrical contact materials. *Trans. Nonferrous Met. Soc. China* **2016**, *26*, 185–195. [CrossRef]

30. Wu, C.; Zhao, Q.; Li, N.; Wang, H.; Yi, D.; Weng, W. Influence of fabrication technology on arc erosion of Ag/10SnO$_2$ electrical contact materials. *J. Alloys Compd.* **2018**, *766*, 161–177. [CrossRef]

31. Li, H.; Wang, X.; Fei, Y.; Zhang, H.; Liu, J.; Li, Z.; Qiu, Y. Effect of electric load characteristics on the arc erosion behavior of Ag-8wt.% Ni electrical contact material prepared by spark plasma sintering. *Sens. Act. Phys.* **2021**, *326*, 112718. [CrossRef]